SUPPLEMENTAL INFORMATION

Fig. S1

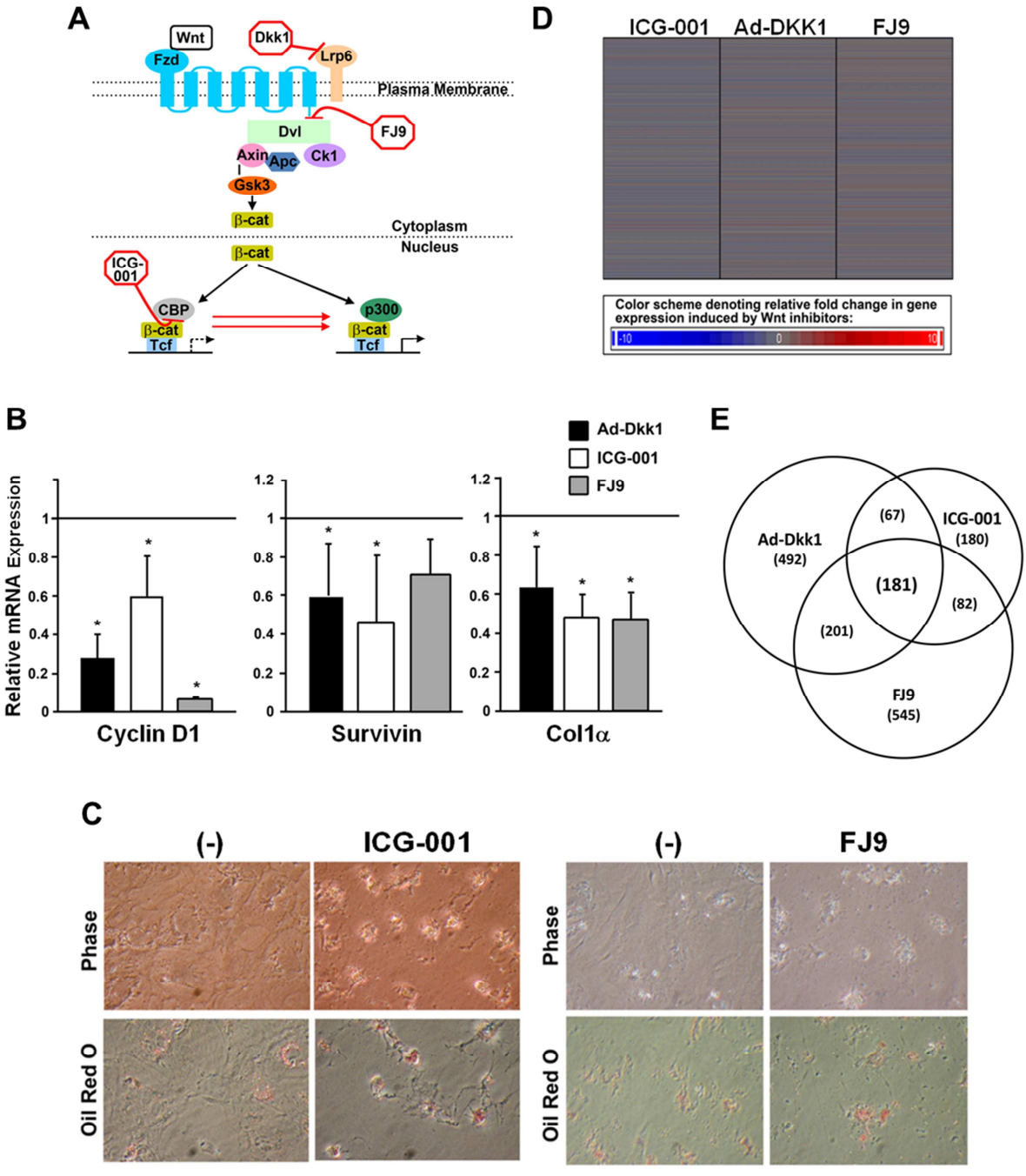

Fig. S1. Canonical Wnt antagonism reverses HSC activation. A. A schematic diagram depicting the sites of action for three inhibitors (Dkk1, FJ9, and ICG-001) of canonical Wnt pathway. DKK-1 blocks the canonical Wnt pathway by binding to LRP5/6 and was previously

used by us to demonstrate the role of the Wnt pathway in HSC activation [1]. FJ9 is an antagonist for Dvl [2] while ICG-001 blocks CBP association with β-catenin [3]. B. All three inhibitors suppress canonical Wnt target genes such as cyclin D1 and survivin, and HSC activation marker *Col1a1*, in cultured primary rat HSCs as compared to the expression level of the respective control set at 1 as indicated by a holizontal line ($n \geq 3$). C. Images of phase contrast microscopy and Oil red O staining of cutured rat HSCs treated with ICG-001 or FJ9. As we have previously demonstrated for DKK-1 [1], ICG-001 and FJ9 morphologically attenuate activated HSCs as shown by retracted HSC morphology and increased Oil red O staining (the latter indicating increased intracellular lipids), the phenotype characteristic of quiescent HSCs. D. A heat map from microarray analysis of culture-activated (7d) HSCs treated with DKK-1, ICG-001, or FJ9 shows only small percentages (3-6%) of the total 27342 genes assayed are differentially regulated ≥1.75 fold by the inhibitors. E. Venn diagram depicting that 181 genes (see Table S1 for list of genes) are commonly suppressed ≥1.75 fold by the three inhibitors.

Fig. S2

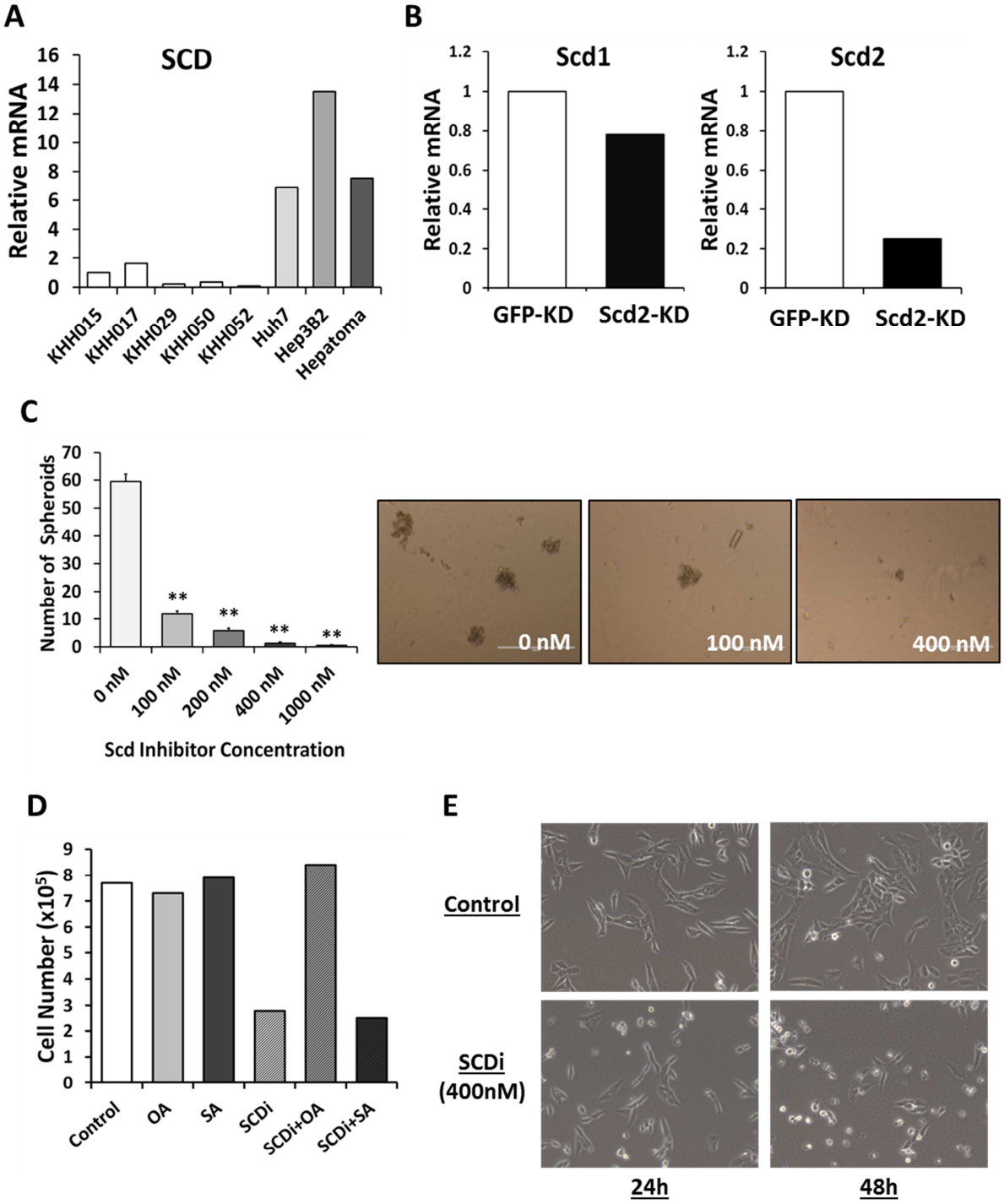

Fig. S2. SCD is induced in human HCC cell lines, and SCD inhibition phenocopies the effects of Scd2-KD on TICs, suppressing their self-renewal in a dose-dependent manner. A.

SCD is induced in 3 human HCC cell lines, Huh7, PLC/PRF/5, and Hep3B vs. normal human hepatocytes, as quantitated by qPCR. B. *Scd2* not *Scd1*, is selectively knocked down (~80%) in a clone of mouse liver TICs stably transduced with lentiviral shRNA targeting *Scd2 (Scd2*-KD*)* vs. a control clone transduced with lentiviral shRNA targeting GFP (GFP-KD). C. Pharmacologic inhibitor SCDi suppresses self-renewal in a dose-dependent manner, as assessed by spheroid formation. At just 400 nM, SCDi almost completely abolishes spheroid formation and drastically reduces spheroid size (n=3). D. SCDi (400 nM) completely abrogates TIC growth at 48 h post-treatment, and this effect is entirely rescued by OA, the product of SCD, but not SA, the substrate of SCD (n=1). This supports not only the specificity of the SCDi used, but also confirms the dependence of TIC self-renewal on SCD's production of OA. E. Morphological analysis reveals a rounded, less-spread, more-quiescent TIC phenotype with SCDi (400 nM) treatment at 48 h, and this effect is entirely rescued by OA but not SA (data not shown).

Fig. S3

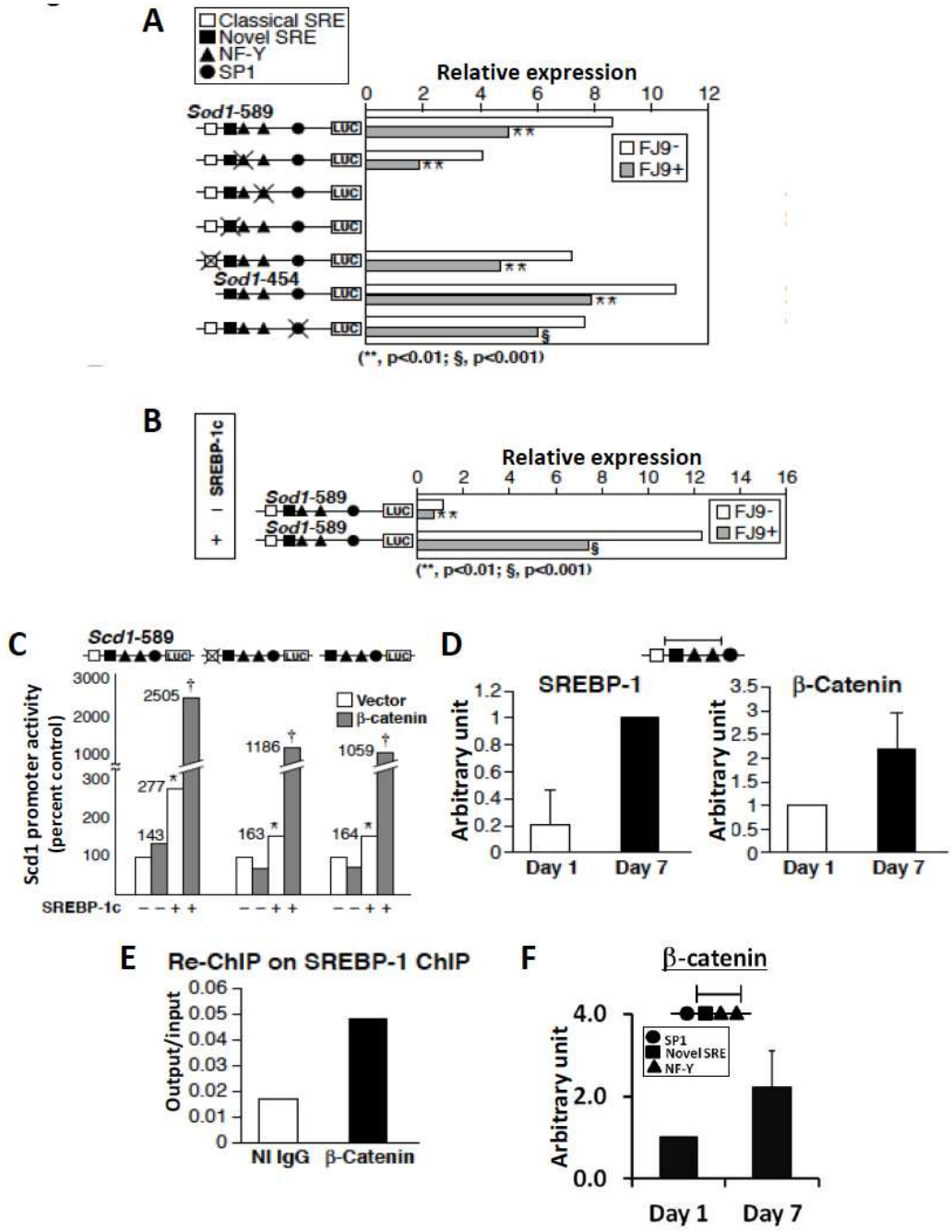

Fig. S3. β-catenin interacts with SREBP-1c to promote Scd1/2 transcription. A. Mouse *Scd1* promoter (-589/+81) with or without various mutations was tested as a luciferase reporter to determine the effects of FJ9 in BSCs. Activities of all constructs are suppressed by FJ9 except for those with novel SRE or proximal NF-Y mutations which abrogate activities, confirming the importance of these two sites. A mutation of the distal NF-Y site reduces the promoter activity

by half. With this mutation or other constructs including that with a mutated or deleted classical SRE, FJ9 still inhibits the promoter activity, suggesting the novel SRE and proximal NF-Y sites are the targets of FJ9. B. *Scd1* promoter activity induced by SREBP-1c is suppressed with FJ9. C. SREBP-1c induced promoter activity is enhanced by β-catenin (n=3). *$p<0.05$ vs. without β-catenin and without SREBP-1c, †$p<0.05$ vs. without β-catenin but with SREBP-1c. D. ChIP-qPCR analysis detects increased enrichments of SREBP-1 and β-catenin at the region with novel SRE/NF-Y elements in day 7 vs. day 1 cells. E. Sequential ChIP analysis detects increased binding of β-catenin to SREBP-1 bound to novel SRE/NF-Y sites in day 7 HSCs. F. ChIP-qPCR analysis for β-catenin shows its enrichment at the region of the mouse *Scd2* proximal promoter with novel SRE/NF-Y sites, in day 7 vs. day 1 HSCs.

Fig. S4

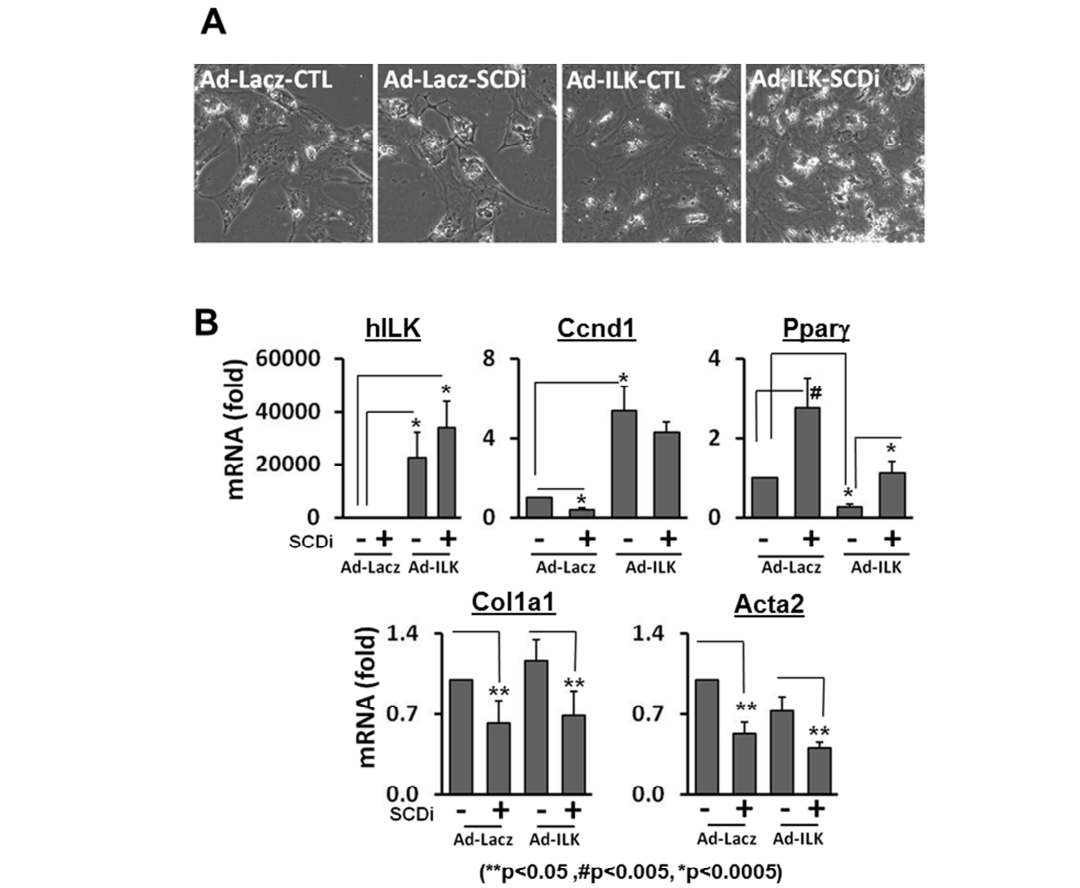
A
Ad-Lacz-CTL
Ad-Lacz-SCDi
Ad-ILK-CTL
Ad-ILK-SCDi
B
hILK
Ccnd1
Pparγ
mRNA (fold)
60000
40000
20000
0
8
4
0
4
2
0
SCDi
- + - +
Ad-Lacz Ad-ILK
Col1a1
Acta2
1.4
0.7
0.0
(**p<0.05 ,#p<0.005, *p<0.0005)
C
CTL
ILKi-1uM
ILKi-2uM
ILKi-3uM
ILKi-3uM+OA
OA
D
CTL
ILKi
OA
ILKi+OA
1.5
1.0
0.5
0.0
Scd1
Scd2
Col1a1

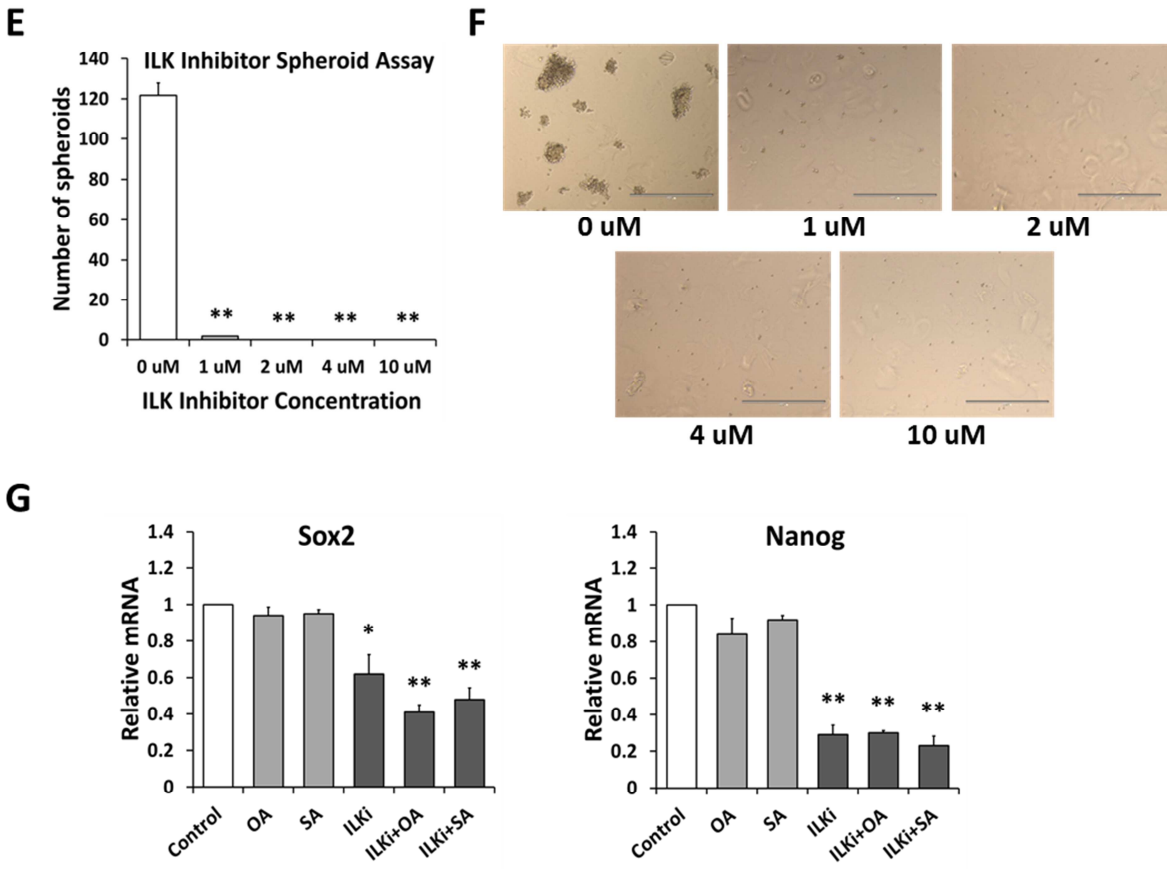

Fig. S4. SCD acts upstream of ILK to promote canonical Wnt pathway. A. The pre-treatment of rat primary culture activated HSCs with Ad-hILK vs. control Ad-LacZ partially prevents SCD inhibitor-induced morphologic reversal to the quiescent state. B. Ad-hILK induces expression of canonical Wnt target gene, *Ccnd1*, and prevents SCD inhibitor-mediated suppression of *Ccnd1* in rat primary culture activated HSCs. Ad-hILK also suppresses HSC quiescence gene *Pparγ*, but this suppression is attenuated by SCD inhibitor-treatment. Interestingly, HSC activation markers, *Col1a1* and *Acta2*, do not appear to be induced by Ad-hILK, but both genes are suppressed by SCD inhibitor-treatment. C. The treatment of rat primary culture-activated HSCs with the cell-permeable ILK inhibitor Cpd 22 (ILKi, 3 μM) results in a morphologic reversal to the quiescent state, but this effect is not rescued by OA. D. Similarly, ILKi-mediated suppression of *Scd1*, *Scd2*, *Col1a1* mRNA levels in rat HSCs are not rescued with OA compared to vehicle-treated control (n=3). E and F. ILKi markedly suppresses TIC's spheroid formation even at a low micromolar range (n=3). G. ILKi also inhibits Sox2 and Nanog expression but these effects are not rescued with OA (n=3). Collectively, these results suggest that SCD exerts its positive regulatory effect at the level upstream of ILK in both HSCs and TICs.

Fig. S5

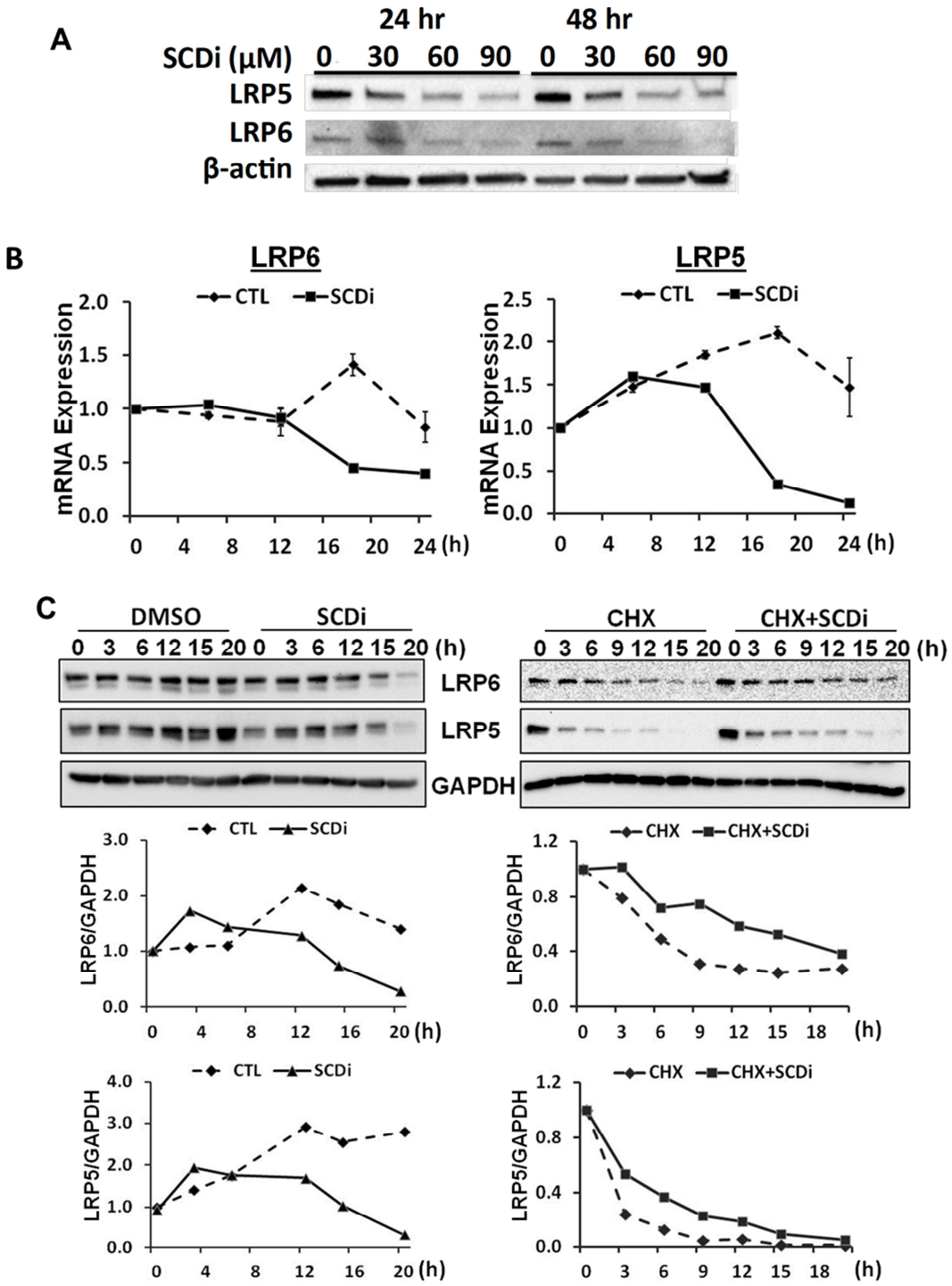
A
24 hr
48 hr
SCDi (μM) 0 30 60 90 0 30 60 90
LRP5
LRP6
β-actin
B
LRP6
LRP5
CTL
SCDi
mRNA Expression
(h)
C
DMSO
SCDi
CHX
CHX+SCDi
LRP6
LRP5
GAPDH
LRP6/GAPDH
LRP5/GAPDH

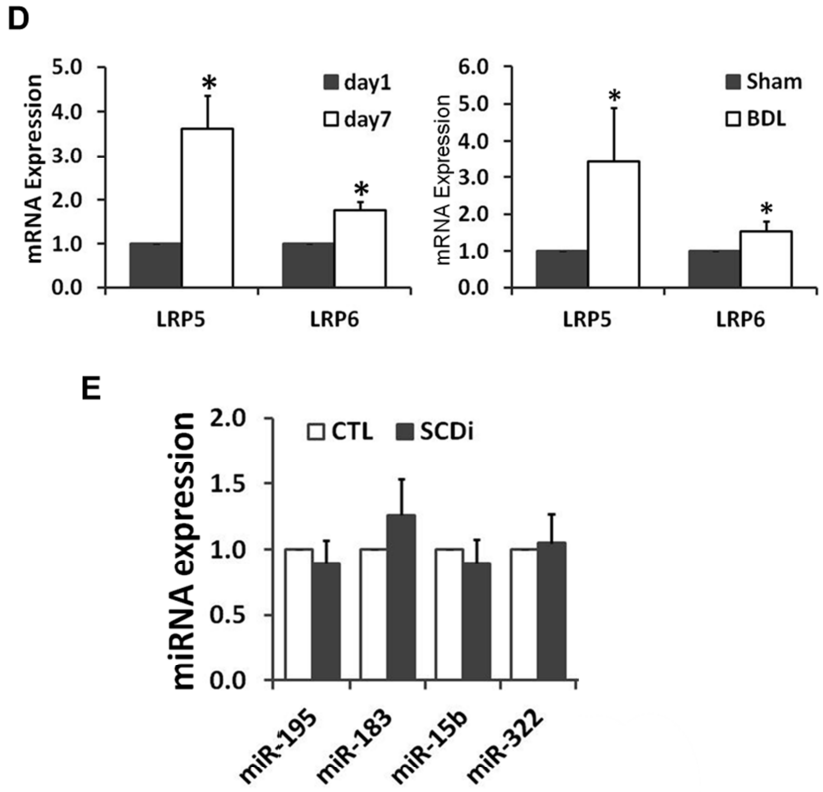

Fig. S5. SCD promotes LRP5/6 expression. A. LRP5/6 repression is evident in SCDi-treated Huh7 cells, similar to what is observed with BSC. B. LRP5 and LRP6 mRNA levels begin to decrease after 12 h of SCDi treatment in BSC. C. Temporal changes in LRP5 and LRP6 proteins were assessed in SCDi- or vehicle (DMSO)-treated BSCs with (right panel) or without (left panel) concomitant treatment with cyclohexamide (CHX, 10 ng/ml). Data from densitometric analysis of LRP5 and LRP6 standardized to GAPDH, are shown in lower graphs of corresponding panels. Without CHX (left panel), SCDi begins to suppress LRP5/6 levels at 12 h after addition of SCDi and progressively depletes both proteins until 20 h. With CHX, both proteins are rapidly degraded until they reach maximally reduced levels at 9 h or thereafter. But the degradation kinetic is not enhanced but rather attenuated with SCDi. D. Induction of Lrp5/6 mRNA in culture- and BDL-activated HSCs confirms functional relevance of these mediators of canonical Wnt pathway in HSC activation. Induction of *Lrp5* and *Lrp6* mRNA levels in activated rat HSCs at day 7 of culture on plastic as quantified by qPCR analysis vs. in quiescent HSCs at day 1 of culture (left panel) (n=3). Similarly, induction of *Lrp5* and *Lrp6* mRNA levels in HSCs isolated from rat livers with biliary liver fibrosis (BDL) vs. in HSCs from control livers (Sham) (right panel) (n=3). E. In-silico algorithms (http://mirdb.org/miRDB/) for screening possible miRNA binding to Lrp6 mRNA 3' UTR predict possible regulation by miR-195, miR-183, miR-15b, and miR-322. But none of these are regulated with SCDi treatment for 15 h as determined by TaqMan-qPCR in BSCs.

Fig. S6

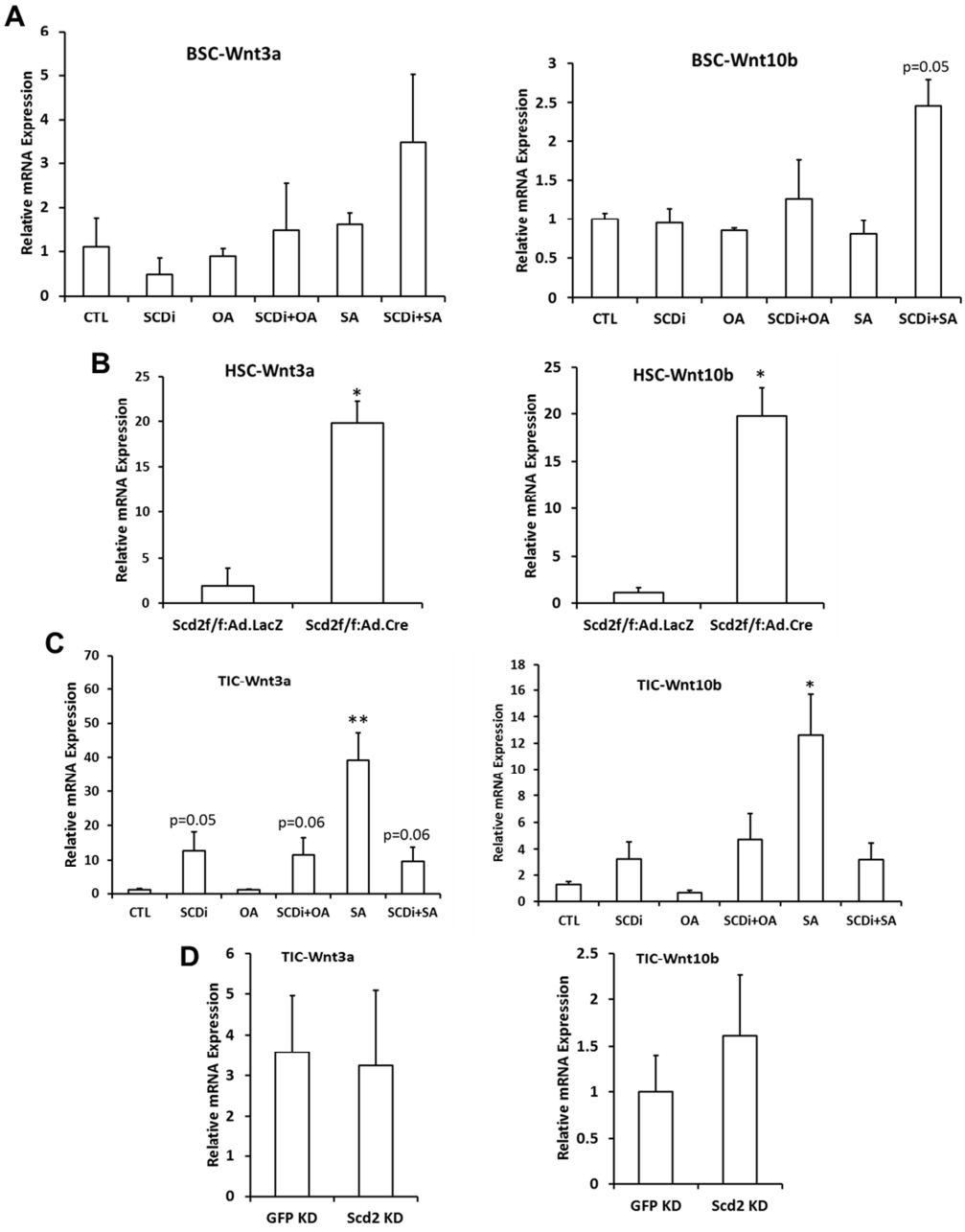

Fig. S6. Unclear effect of SCD inhibition or Scd2 KD on canonical Wnt3a and Wnt10b in BSCs, HSCs, and TICs. A. SCDi+SA tends to increase Wnts3a and 10b in BSC (n=4). B. Scd2 KD induces Wnts3a and 10b in Scd2f/f;Ad.Cre HSCs (n=3). C. SA induces Wnts 3a and 10b in TICs (n=3). D. Scd2 KD does not appear to affect Wnts3a and 10b in TICs (n=3). Error bars represent SEM.

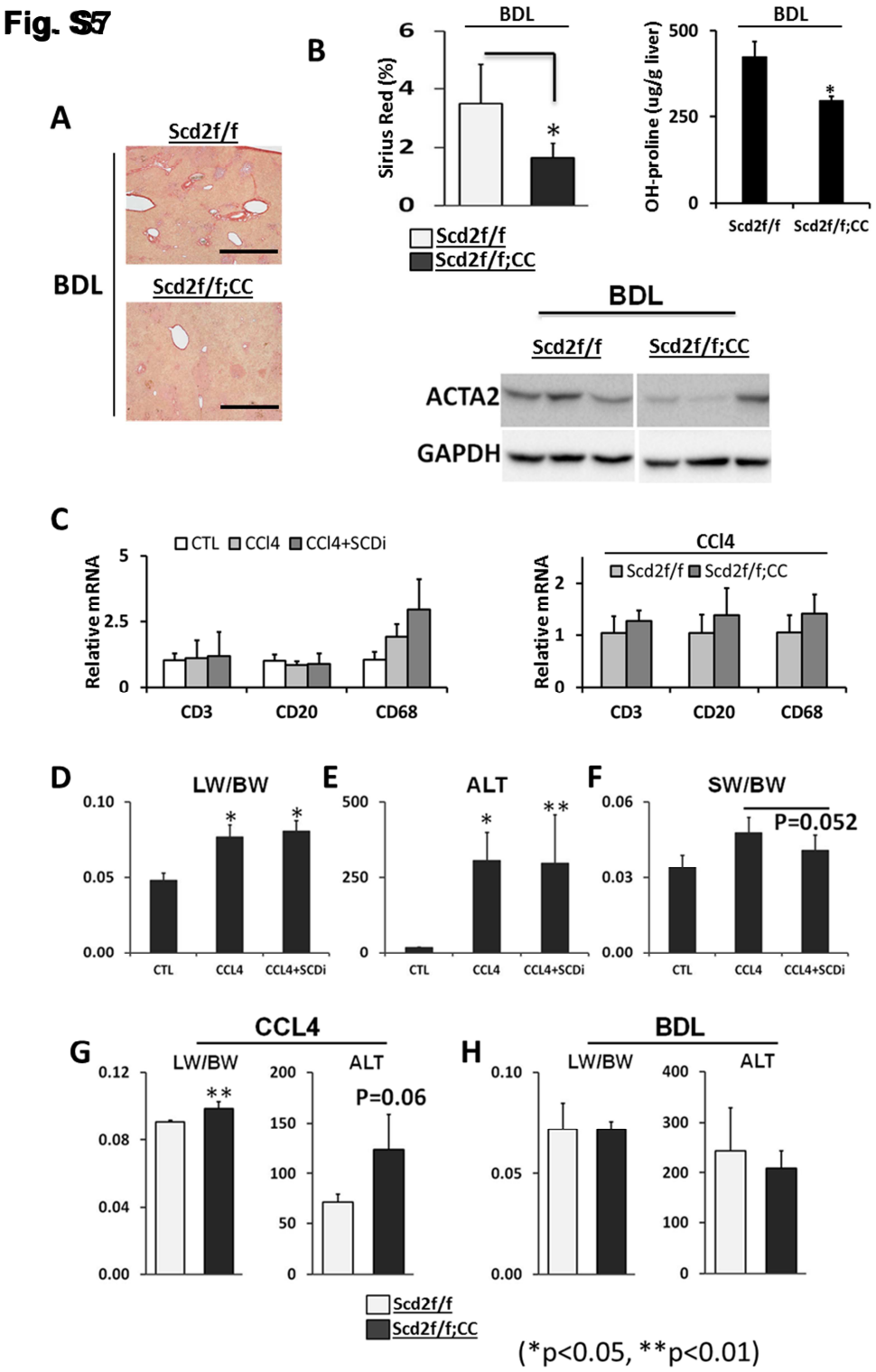

Fig. S7. HSC-specific Scd2 deletion (Scd2flox/flox:CC) ameliorates liver fibrosis in BDL mouse model. A. *Scd2*$^{flox/flox}$*:CC* vs. *Scd2*$^{flox/flox}$ (control) mice were subjected to BDL and euthanized 12 d later. Fibrosis is suppressed in livers of HSC-specific *Scd2* deleted BDL mice

vs control BDL mice, as evidence by decreased Sirius Red staining. B. HSC-specific *Scd2* deleted mice (n=5) show reduced liver fibrosis as assessed by morphometry for Sirius red and hydroxyproline content (top), and decreased hepatic levels of α-smooth muscle actin (Acta2) (bottom). C. Major immune cell subsets of T-, B-, and myeloid cells were assessed by qPCR for CD3, CD20, CD68, respectively, of liver tissues from CCl4 models of fibrosis, but no difference was found between groups with or without SCD suppression. (n=6.) D, E, and F. SCDi treatment does not affect liver weight/body weight ratio or plasma ALT levels in CCl4-treated mice but tends to reduce spleen weight/body weight ratio, suggesting the treatment unlikely influenced underlying toxic injury, yet still reduced the severity of liver fibrosis and splenomegaly. (n=6.) G and H. *Scd2* gene ablation (*Scd2*flox/flox:*CC*) increases liver weight/body weight ratio and plasma ALT in the CCl4 model but not in BDL model, indicating worsened CCl4 hepatotoxicity due to Scd2 deficiency in HSCs. (n=5-6.) Error bars represent SEM (B,D-H).

Supplemental Tables

Table S1 – *GENE LIST:* A list of genes commonly suppressed by at least 1.75 fold in cultured primary rat hepatic stellate cells across Dkk1, ICG-001, and FJ9 treatments (Tx), and ordered by mean fold change (FC) of all 3 treatments. Seven-day cultured hepatic stellate cells were infected with an adenovirus expressing DKK-1 or GFP; or treated with FJ9, ICG-001, or respective vehicle for 24 hr in serum-free DMEM. Total RNA extracted was analyzed by Affymetrix Rat Gene 1.0 ST Array kit according to the manufacturer's protocol. (--- = unidentified)

Probeset ID	Gene Symbol	Gene Name	Dkk1 Tx FC	ICG Tx FC	FJ9 Tx FC	Mean FC for 3 Tx
10753425	Mx1	myxovirus (influenza virus) resistance 1	-9.39	-11.61	-16.26	-12.42
10715546	Scd2	stearoyl-Coenzyme A desaturase 2	-2.34	-2.56	-19.69	-8.20
10934865	Srpx2 (predicted)	sushi-repeat-containing protein, X-linked 2	-2.73	-11.87	-9.31	-7.97
10819500	---	---	-4.85	-5.69	-12.28	-7.61
10928837	Igfbp5	insulin-like growth factor binding protein 5	-10.91	-4.71	-4.13	-6.58
10908521	Ldlr	low density lipoprotein receptor	-2.21	-1.77	-14.89	-6.29
10791358	Ddx60	DEAD (Asp-Glu-Ala-Asp) box polypeptide 60	-4.96	-3.41	-9.78	-6.05
10709687	Olfml1	olfactomedin-like 1	-2.79	-1.91	-13.30	-6.00
10765444	---	---	-8.09	-7.40	-2.42	-5.97
10851350	Tgm2	transglutaminase 2, C polypeptide	-3.00	-3.30	-11.52	-5.94
10857382	Fgd5 (predicted)	FYVE, RhoGEF and PH domain containing 5	-3.14	-6.98	-7.70	-5.94
10728631	Fads2	fatty acid desaturase 2	-3.42	-5.81	-8.39	-5.87
10799241	Idi1	isopentenyl-diphosphate delta isomerase	-1.89	-3.65	-11.86	-5.80
10787889	Ddx60	DEAD (Asp-Glu-Ala-Asp) box polypeptide 60	-5.21	-3.27	-8.80	-5.76
10711979	Gpr123 (predicted)	G protein-coupled receptor 123	-2.61	-7.15	-6.37	-5.38
10764244	Tnnt2	troponin T2, cardiac	-2.82	-9.59	-3.52	-5.31
10791394	---	---	-4.58	-2.75	-8.36	-5.23
10801975	MGC108823	similar to interferon-inducible GTPase	-5.86	-3.58	-6.12	-5.19
10769672	Rgs4	regulator of G-protein signaling 4	-6.56	-5.53	-3.44	-5.18
10792344	Sfrp1	secreted frizzled-related protein 1	-3.39	-4.78	-7.28	-5.15
10826249	Vcam1	vascular cell adhesion molecule 1	-7.05	-3.86	-4.25	-5.05
10730349	Scd1	stearoyl-Coenzyme A desaturase 1	-4.42	-6.40	-4.27	-5.03
10793080	Gdf2	growth differentiation factor 2	-5.74	-2.81	-6.47	-5.01

10733056	Ifi47	interferon gamma inducible protein 47	-4.17	-4.40	-6.15	-4.91
10889399	Rsad2	radical S-adenosyl methionine domain containing 2	-4.12	-3.20	-7.18	-4.83
10714745	Il33	interleukin 33	-3.81	-3.67	-6.96	-4.81
10823949	Lrat	lecithin-retinol acyltransferase	-2.38	-2.70	-8.93	-4.67
10929458	Sphkap	SPHK1 interactor, AKAP domain containing	-3.50	-3.39	-7.03	-4.64
10886621	Serpina3n	serine (or cysteine) peptidase inhibitor, clade A, mem	-8.59	-2.45	-2.77	-4.60
10859090	LOC689800	similar to osteoclast inhibitory lectin	-3.45	-5.25	-4.98	-4.56
10825559	LOC690430	similar to nuclear receptor subfamily 1, grou	-4.98	-5.03	-3.64	-4.55
10765437	Rgs5	regulator of G-protein signaling 5	-7.34	-4.15	-2.08	-4.53
10764005	Plekha6 (predicted)	pleckstrin homology domain containing, family	-3.71	-2.42	-7.34	-4.49
10813214	Hmgcs1	3-hydroxy-3-methylglutaryl-Coenzyme A synthase 1	-2.25	-3.01	-8.07	-4.44
10937725	Figf	c-fos induced growth factor	-3.04	-2.97	-6.77	-4.26
10702913	Fndc1	fibronectin type III domain containing 1	-2.81	-1.76	-7.99	-4.18
10728123	Tm7sf2	transmembrane 7 superfamily member 2	-3.63	-6.14	-2.41	-4.06
10702945	Acat2	acetyl-Coenzyme A acetyltransferase 2	-2.57	-3.14	-6.32	-4.01
10895083	Lum	lumican	-3.63	-2.44	-5.84	-3.97
10866512	Mgp	matrix Gla protein	-4.31	-4.51	-3.00	-3.94
10763604	Gpr39	G protein-coupled receptor 39	-2.23	-3.41	-5.65	-3.77
10858165	Cxcl12	chemokine (C-X-C motif) ligand 12	-2.72	-2.22	-6.22	-3.72
10755088	Rtp4 (predicted)	receptor transporter protein 4	-3.88	-2.47	-4.64	-3.66
10742868	LOC686661	similar to CG1998-PA	-3.71	-2.31	-4.84	-3.62
10870567	Dhcr24	24-dehydrocholesterol reductase	-2.71	-3.22	-4.67	-3.53
10722247	E2f8	E2F transcription factor 8	-5.08	-2.90	-2.61	-3.53
10749762	Sectm1b	secreted and transmembrane 1B	-4.16	-3.84	-2.58	-3.53
10758777	Oas1a	2'-5' oligoadenylate synthetase 1A	-3.26	-2.12	-5.17	-3.52
10796683	RGD1563437 (predicted)	similar to KIAA1217	-1.97	-2.41	-6.12	-3.50
10861811	RGD1308013 (predicted)	similar to hypothetical protein B230314O	-5.87	-1.93	-2.66	-3.49
10861835	Ptn	pleiotrophin	-3.10	-5.50	-1.81	-3.47
10827094	Gbp1 (predicted)	guanylate binding protein 1, interferon-	-3.29	-1.76	-5.30	-3.45
10883960	Cmpk2	cytidine monophosphate (UMP-CMP) kinase 2, mitochondria	-3.93	-3.29	-3.06	-3.43
10737205	Sept4	septin 4	-1.88	-2.29	-5.87	-3.35

10708896	Garp (predicted)	glycoprotein A repetitions predominant	-2.50	-1.76	-5.77	-3.34
10841348	Acss2 (predicted)	acyl-CoA synthetase short-chain family member	-2.79	-3.76	-3.36	-3.30
10796679	LOC681362	similar to p130Cas-associated protein (p140Cap) (SN	-1.89	-2.16	-5.86	-3.30
10819005	Elovl6	ELOVL family member 6, elongation of long chain fatty aci	-1.81	-3.93	-4.14	-3.29
10714903	Ifit3	interferon-induced protein with tetratricopeptide repea	-4.02	-3.04	-2.78	-3.28
10757726	Eln	elastin	-3.40	-4.43	-1.99	-3.27
10909639	Fxyd6	FXYD domain-containing ion transport regulator 6	-3.04	-2.35	-4.38	-3.25
10713857	Fads1	fatty acid desaturase 1	-3.48	-2.97	-3.29	-3.25
10861678	Plxna4 (predicted)	plexin A4	-3.21	-3.69	-2.81	-3.24
10714907	Ifit1	interferon-induced protein with tetratricopeptide repeats	-1.86	-2.18	-5.65	-3.23
10770807	G0s2	G0/G1 switch gene 2	-5.05	-2.50	-2.11	-3.22
10911797	Gsta4	glutathione S-transferase, alpha 4	-5.14	-2.52	-1.80	-3.15
10731047	Ablim1 (predicted)	actin-binding LIM protein 1	-2.45	-2.64	-4.33	-3.14
10888953	Emilin1 (predicted)	elastin microfibril interfacer 1	-2.02	-3.14	-4.24	-3.14
10857358	Fgd5 (predicted)	FYVE, RhoGEF and PH domain containing 5	-2.31	-3.49	-3.54	-3.11
10762747	Oasl2	2'-5' oligoadenylate synthetase-like 2	-3.06	-2.14	-4.14	-3.11
10751295	Pla1a	phospholipase A1 member A	-4.06	-1.78	-3.44	-3.09
10776459	Pdgfra	platelet derived growth factor receptor, alpha polypeptid	-2.42	-4.26	-2.51	-3.06
10771655	Cxcl10	chemokine (C-X-C motif) ligand 10	-3.78	-2.15	-3.21	-3.05
10712560	Dhcr7	7-dehydrocholesterol reductase	-2.80	-2.21	-4.05	-3.02
10912088	Nt5e	5' nucleotidase, ecto	-3.64	-3.35	-1.98	-2.99
10749768	Sectm1a	secreted and transmembrane 1A	-4.84	-2.09	-1.99	-2.97
10882525	Tmem178	transmembrane protein 178	-2.71	-3.41	-2.76	-2.96
10880095	Serinc2	serine incorporator 2	-3.68	-3.26	-1.93	-2.95
10913095	Ube1l (predicted)	ubiquitin-activating enzyme E1-like	-4.66	-2.24	-1.92	-2.94
10866724	Abcc9	ATP-binding cassette, sub-family C (CFTR/MRP), member 9	-3.03	-1.83	-3.91	-2.92
10832378	Lss	lanosterol synthase	-2.09	-3.16	-3.49	-2.91
10929766	Col6a3 (predicted)	procollagen, type VI, alpha 3	-3.29	-3.19	-2.24	-2.91
10769680	Hsd17b7	hydroxysteroid (17-beta) dehydrogenase 7	-2.40	-2.38	-3.93	-2.91
10896772	Sqle	squalene epoxidase	-2.22	-2.28	-4.13	-2.88
10763976	Plekha6	pleckstrin homology domain	-3.02	-1.81	-3.81	-2.88

	(predicted)	containing				
10917205	---	---	-3.38	-1.80	-3.46	-2.88
10912051	Prss35	protease, serine, 35	-2.42	-2.18	-3.98	-2.86
10749340	St6galnac1	ST6 (alpha-N-acetyl-neuraminyl-2,3-beta-galactosyl	-2.01	-1.98	-4.59	-2.86
10932610	RGD1561594 (predicted)	similar to testis-specific farnesyl pyropho	-1.87	-2.67	-4.04	-2.86
10827809	RT1-S3	RT1 class Ib, locus S3	-3.04	-2.12	-3.41	-2.85
10823093	Osap	ovary-specific acidic protein	-2.73	-2.86	-2.95	-2.85
10702955	RGD1562948 (predicted)	similar to Ab2-076	-2.49	-2.51	-3.54	-2.85
10927842	Stat1	signal transducer and activator of transcription 1	-2.89	-1.92	-3.67	-2.82
10853931	LOC500046	similar to hypothetical protein FLJ21986	-2.89	-2.43	-3.08	-2.80
10860597	Steap4	STEAP family member 4	-2.46	-2.02	-3.91	-2.80
10724902	Mrvi1 (predicted)	MRV integration site 1 homolog (mouse)	-2.12	-2.45	-3.79	-2.78
10889446	---	---	-4.31	-1.98	-2.05	-2.78
10759989	RGD1307396 (predicted)	similar to RIKEN cDNA 6330406I15	-2.46	-1.93	-3.92	-2.77
10753279	Erg	avian erythroblastosis virus E-26 (v-ets) oncogene related	-2.95	-2.08	-3.29	-2.77
10744597	LOC691995	hypothetical protein LOC691995	-3.43	-3.04	-1.81	-2.76
10855416	Tmem176a	transmembrane protein 176A	-2.81	-2.81	-2.62	-2.75
10743774	Ntn1	netrin 1	-2.23	-1.96	-4.00	-2.73
10759198	Cmklr1	chemokine-like receptor 1	-1.96	-1.86	-4.33	-2.71
10813872	Cdh18 (predicted)	cadherin 18, type 2	-2.56	-2.03	-3.51	-2.70
10881424	Tnfrsf1b	tumor necrosis factor receptor superfamily, member 1b	-3.72	-2.39	-1.97	-2.69
10754563	Itgb5	integrin, beta 5	-2.37	-2.25	-3.45	-2.69
10760080	Rasl11a	RAS-like family 11 member A	-2.69	-1.96	-3.36	-2.67
10729377	Mamdc2	MAM domain containing 2	-3.73	-2.50	-1.77	-2.67
10756418	Flt1	FMS-like tyrosine kinase 1	-3.04	-2.34	-2.61	-2.67
10823278	Tm4sf1 (predicted)	transmembrane 4 superfamily member 1	-1.94	-1.84	-4.14	-2.64
10929321	RGD1561963 (predicted)	similar to Dedicator of cytokinesi	-2.91	-2.21	-2.77	-2.63
10804567	Synpo	synaptopodin	-2.25	-2.56	-3.06	-2.62
10853471	Cyp51	cytochrome P450, subfamily 51	-1.86	-2.10	-3.86	-2.61
10932891	LOC681355	similar to potassium channel tetramerisation	-2.91	-2.05	-2.86	-2.61
10855727	Adcyap1r1	adenylate cyclase activating polypeptide 1 receptor 1	-3.02	-2.31	-2.43	-2.59
10839598	RGD1304904 (predicted)	similar to mitochondrial glycerol	-3.27	-2.14	-2.35	-2.58
10765600	F11r	F11 receptor	-2.85	-2.16	-2.73	-2.58
10735891	RGD1562631 (predicted)	similar to RIKEN cDNA 2010305C02	-3.02	-2.19	-2.52	-2.57

10739927	C1qtnf1	C1q and tumor necrosis factor related protein 1	-2.24	-2.91	-2.52	-2.56
10751469	Parp14	poly (ADP-ribose) polymerase family, member 14	-2.46	-1.95	-3.18	-2.53
10798135	Serpinb9	serine (or cysteine) peptidase inhibitor, clade B, m	-2.53	-2.45	-2.60	-2.53
10714353	Tmem2 (predicted)	transmembrane protein 2	-3.36	-1.82	-2.33	-2.50
10759177	Tmem119	transmembrane protein 119	-1.93	-1.91	-3.65	-2.50
10912277	LOC367140	similar to Heterogeneous nuclear ribonucleoprotein A1	-1.84	-3.30	-2.35	-2.50
10704728	Dmpk (predicted)	dystrophia myotonica-protein kinase	-1.76	-3.08	-2.65	-2.50
10799548	Ccdc3	coiled-coil domain containing 3	-2.90	-2.21	-2.28	-2.46
10897405	Apol3	apolipoprotein L, 3	-3.06	-2.04	-2.24	-2.45
10777468	Ablim2	actin-binding LIM protein 2	-2.82	-2.33	-2.15	-2.43
10862403	Rarres2	retinoic acid receptor responder (tazarotene induced)	-3.36	-1.80	-2.15	-2.43
10702194	Tmem200a	transmembrane protein 200A	-1.81	-2.90	-2.59	-2.43
10738972	Mrc2	mannose receptor, C type 2	-2.33	-2.24	-2.72	-2.43
10921532	Ptk7 (predicted)	PTK7 protein tyrosine kinase 7	-3.46	-1.96	-1.86	-2.42
10859117	---	---	-2.60	-2.05	-2.60	-2.41
10838242	Wt1	Wilms tumor 1	-3.04	-2.42	-1.77	-2.41
10738391	Aoc3	amine oxidase, copper containing 3	-1.98	-2.97	-2.26	-2.40
10726172	Fgfr2	fibroblast growth factor receptor 2	-2.32	-1.98	-2.90	-2.40
10729009	Dtx4	deltex 4 homolog (Drosophila)	-2.33	-2.00	-2.85	-2.40
10853554	Gng11	guanine nucleotide binding protein (G protein), gamma 11	-1.91	-2.09	-3.13	-2.38
10813445	Lifr	leukemia inhibitory factor receptor	-2.82	-1.82	-2.47	-2.37
10766835	Plxna2 (predicted)	plexin A2	-2.74	-1.89	-2.42	-2.35
10734242	Mfap4	microfibrillar-associated protein 4	-2.71	-2.21	-2.05	-2.32
10839596	Adra2b	adrenergic receptor, alpha 2b	-2.65	-1.77	-2.43	-2.28
10919422	Acpl2	acid phosphatase-like 2	-1.94	-2.02	-2.89	-2.28
10803991	Cd14	CD14 antigen	-1.86	-2.17	-2.77	-2.27
10708521	Ctsc	cathepsin C	-3.23	-1.80	-1.77	-2.27
10898968	Pfkm	phosphofructokinase, muscle	-1.99	-2.64	-2.16	-2.27
10878210	Kank4	KN motif and ankyrin repeat domains 4	-2.38	-2.42	-1.99	-2.26
10802338	Ccbe1 (predicted)	collagen and calcium binding EGF domain	-2.51	-2.21	-2.02	-2.25
10777232	Cd38	CD38 antigen	-2.25	-1.82	-2.63	-2.23
10891297	RGD1310769 (predicted)	similar to HSPC288	-1.90	-2.19	-2.57	-2.22

10810591	Fhod1	formin homology 2 domain containing 1	-2.03	-2.09	-2.49	-2.20
10866718	Kcnj8	potassium inwardly-rectifying channel, subfamily J, member	-2.38	-1.77	-2.40	-2.18
10844248	---	---	-2.18	-2.13	-2.22	-2.18
10729777	Ch25h	cholesterol 25-hydroxylase	-2.61	-1.95	-1.97	-2.18
10931154	Dbi	diazepam binding inhibitor	-1.88	-2.17	-2.46	-2.17
10883903	Rrm2	ribonucleotide reductase M2	-2.39	-2.21	-1.86	-2.15
10775731	Cxcl13	chemokine (C-X-C motif) ligand 13	-2.06	-2.01	-2.35	-2.14
10762740	Oasl1	2'-5' oligoadenylate synthetase-like 1	-1.90	-2.55	-1.94	-2.13
10825665	Capza1	capping protein (actin filament) muscle Z-line, alpha	-2.29	-1.92	-2.16	-2.12
10757129	Pdgfa	platelet derived growth factor, alpha	-2.21	-1.84	-2.26	-2.11
10817057	S100a4	S100 calcium-binding protein A4	-1.77	-2.24	-2.27	-2.10
10760290	Nptx2	neuronal pentraxin 2	-1.89	-2.13	-2.27	-2.10
10935031	MGC109340	similar to Microsomal signal peptidase 23 kDa subunit	-2.10	-1.82	-2.30	-2.07
10769825	Fcer1g	Fc receptor, IgE, high affinity I, gamma polypep	-2.35	-1.78	-2.05	-2.06
10729825	Htr7	5-hydroxytryptamine (serotonin) receptor 7	-1.77	-2.05	-2.31	-2.05
10732750	Slit3	slit homolog 3 (Drosophila)	-1.86	-2.32	-1.94	-2.04
10810144	Rrm2	ribonucleotide reductase M2	-2.02	-2.25	-1.85	-2.04
10786710	Btd	biotinidase	-1.86	-2.24	-1.93	-2.01
10860372	---	---	-2.27	-1.78	-1.93	-1.99
10891880	Prima1 (predicted)	proline rich membrane anchor 1	-2.02	-2.08	-1.86	-1.99
10724131	Il18bp	interleukin 18 binding protein	-2.31	-1.80	-1.80	-1.97
10826828	Hadh	hydroxyacyl-Coenzyme A dehydrogenase	-2.16	-1.75	-1.99	-1.97
10765105	---	---	-1.79	-2.09	-1.94	-1.94
10930738	Oit3	oncoprotein induced transcript 3	-1.85	-1.87	-2.09	-1.94
10851599	Sdc4	syndecan 4	-1.82	-1.82	-2.09	-1.91
10870261	Ak3l1	adenylate kinase 3-like 1	-1.88	-1.97	-1.88	-1.91
10744709	Smtnl2	smoothelin-like 2	-1.95	-1.81	-1.90	-1.89
10766760	LOC679692	similar to lysophosphatidylglycerol acyltransferase	-1.78	-1.82	-1.92	-1.84
10862649	Nod1	nucleotide-binding oligomerization domain containing 1	-1.87	-1.77	-1.79	-1.81
10829713	Bicc1 (predicted)	bicaudal C homolog 1	-1.88	-1.76	-1.78	-1.81
10907952	Tmem123	transmembrane protein 123	-1.77	-1.77	-1.79	-1.78

Table S2 *– FATTY ACID CONTENT:* Fatty acid content in total lipid extracts from day 1 quiescent and day 7 activated cultured HSCs. Fatty acids are quantified by GC/MS with heptadecanoic acid (17:0) as an internal standard. Data are presented as mean ± SD of nmol/million cells of the fatty acids. * $p < 0.05$ comparing to Day 1 cells; # $p < 0,05$ compared to solvent control treatment.

Fatty Acid	**Day 1 HSCs (nmol/million cells)**	**Day 7 HSCs (nmol/million cells)**		
		Control	**Solvent control**	**FJ9 (200uM)**
C14:0	1.41 ± 0.05	9.18 ± 1.22 *	7.96 ± 1.26	3.59 ± 1.13 #
C16:0	371.9 ± 79.8	721.1 ± 166.4 *	563.5 ± 153.7	347.6 ± 160.2
C16:1 (n-7)	2.21 ± 0.16	19.38 ± 3.35 *	17.21 ± 2.74 *	4.05 ± 2.31 #
C18:0	94.3 ± 16.8	258.8 ± 41.3 *	214.5 ± 12.5 *	137.3 ± 45.5 #
C18:1 (n-9)	24.8 ± 3.56	145.3 ± 39.1 *	121.3 ± 35.9 *	38.6 ± 20.5 #
C18:1 (n-7)	11.9 ± 1.76	65.9 ± 21.1 *	40.5 ± 2.58 *	22.6 ± 13.9 #
C18:2 (n-6)	26.8 ± 3.10	45.7 ± 12.9 *	34.8 ± 9.86	18.3 ± 10.4
C20:0	0.40 ± 0.05	3.11 ± 1.21 *	2.19 ± 0.14 *	1.30 ± 0.76
C20:4 (n-6)	16.7 ± 1.29	88.9 ± 35.1 *	63.8 ± 13.8 *	29.9 ± 17.4 #
C22:0	0.45 ± 0.13	2.75 ± 0.67 *	2.37 ± 0.35 *	1.19 ± 0.29 #
C22:1	0.40 ± 0.06	4.49 ± 1.23	4.68 ± 0.38	1.43 ± 0.17
C24:0	0.63 ± 0.29	7.01 ± 1.43 *	4.81 ± 1.32 *	1.24 ± 0.83 #

Supplemental Methods

Human liver biopsy tissues and human hepatocytes. Human liver biopsy tissues were obtained from Histopathology and Tissue Shared Resource, Georgetown University, and tissues were immunohistochemically stained and semi-quantitatively assessed for SCD as previously described[5]. Human hepatocytes from liver donors were isolated as previously described[6] and obtained from Pharmacology, Toxicology and Therapeutics Dept, University of Kansas Medical Center.

Patient cohort for bioinformatics analysis of gene expression profiling data to correlate SCD expression with clinical outcome in HCC at the population level. The cohort of HCC patients (n=242) used for our bioinformatics analysis has previously been clinically characterized[7] with >90% of patients suffering from hepatitis B virus infection which is the most frequent cause of HCC worldwide.

BSC line. A spontaneously immortalized HSC line, designated as BSC, was established from activated HSC isolated from experimental biliary liver fibrosis as previously described [8] and maintained in low glucose DMEM with 5% FBS and antibiotics.

SCD inhibitor, ILK inhibitor, and Porcupine inhibitor treatment of HSCs/BSCs or TICs/Huh7. Pharmacologic inhibitors of SCD (A939572 from BioVision) (1-2 μM), ILK (Cpd22 from Calbiochem) (1-3 μM), and Porcupine (LGK974 from StemRD) (0.5 μM) or vehicle control were used to treat HSCs/BSCs in serum-free medium from 20-96 h unless otherwise indicated. Prior to treatment with inhibitor, HSCs/BSCs were washed with serum free medium twice. Cells were replenished with fresh inhibitor or vehicle every 48 h when applicable (for treatments >2 days). SCD inhibitor 100-1000 nM for TICs or 20-90 uM for Huh7 was used for treatment from 24-48 h unless otherwise indicated.

Preparation of BSA-conjugated fatty acids and treatment of HSCs/BSCs or TICs/Huh7. Oleic acid (O1008), stearic acid (S4751), palmitic acid (P0500), and palmitoleic acid (P9417), and fatty acid free-BSA (A8806) were purchased from Sigma. BSA-conjugated fatty acids were prepared by diluting 50 mM stock fatty acids in DMSO with 100 mg/ml BSA in 1x PBS to produce a 3 mM working solution. Cells were then treated with a final concentration of 30 μM BSA-conjugated fatty acid (and a final concentration of 0.1% BSA) or vehicle control. Cells were replenished with fresh BSA-conjugated fatty acid or vehicle every 48 h when applicable (for treatments >2 days).

RNA extraction and RT-qPCR. Total RNA was extracted from HSCs/BSCs or liver TICs/HCC cell lines or normal hepatocytes using the Quick-RNA MiniPrep (Zymo Research) or Direct-zol RNA MiniPrep Kit (Zymo Research). For RT-qPCR, cDNAs were synthesized from 1 μg total RNA using the Maxima First Strand Synthesis Kit for RT-qPCR (Thermo Scientific). Quantitative PCR was performed where cDNA was amplified for 40 cycles using the SYBR Green PCR master mix (Applied Biosystems) and the ViiA 7 Real-Time PCR System (Applied Biosystems). Each threshold cycle (Ct) value was first normalized to the 36B4 (Rplp0) Ct value of a sample and subsequently to a control sample.

Primer sequences. Primer sequences used for RT-qPCR, ChIP assay.

RT-qPCR primers	Species	Forward Primer Sequence (5'->3')	Reverse Primer Sequence (5'->3')
Acta2	rat	TGTGCTGGACTCTGGAGATG	GATCACCTGCCCATCAGG
Acta2	mouse	CTGAGCGTGGCTATTCCTTC	CTTCTGCATCCTGTCAGCAA
Birc5	rat	GTACCTTAAGGACCACCGGATC	GTCATCCGGTTCCCAGCCTTCC
Ccnd1	rat, mouse	TGGAACTGCTTCTGGTGAAC	TTCACATCTGTGGCACAGAG
Col1a1	rat	TCGATTCACCTACAGCACGC	GACTGTCTTGCCCCAAGTTCC
Col1a1	mouse	CACCACCCTCAAGAGCCTGAGTC	GTTCGGGCTGATGTACCAGT
Lrp5	rat	GCCATCGACTATGACCCACT	CTCGGTGTTCACAAGGGTC
Lrp6	rat	TGGATCTGGCAGTCAGTTTG	CGATCAGTGCCAGTGTCTG
Nanog	mouse	AGGGTCTGCTACTGAGATGCTCTG	CAACCACTGGTTTTTCTGCCACCG
Pparg	rat	CCTGAAGCTCCAAGAATACCAAA	AGAGTTGGGTTTTTTCAGAATAATAAGG
Pparg	mouse	AAGAGCTGACCCAATGGT	ATGGTTCTTCGGAAAAAA

RPLP0	human	CAGATTGGCTACCCAACTGTT	GGAAGGTGTAATCCGTCTCCAC
Rplp0	rat	TTCCCACTGGCTGAAAAGGT	CGCAGCCGCAAATGC
Rplp0	mouse	AGATTCGGGATATGCTGTTGGC	TCGGGTCCTAGACCAGTGTTC
SCD	human	GCAGGACGATATCTCTAGCT	GTCTCCAACTTATCTCCTCCATTC
Scd1	rat	TACACTCTGGTGCTCAACGC	AGGATGTTCTCCCGAGATTG
Scd1	mouse	GCGATACACTCTGGTGCTCA	CCCAGGGAAACCAGGATATT
Scd2	rat	TCCTGCTCATGTGCTTCATC	TCTCCCGAGAGCTGATGTTC
Scd2	mouse	GCTCTCGGGAGAACATCTTG	CAGCCCTGGACACTCTCTTC
Sox2	mouse	GGCAGCTACAGCATGATGCAGGAG C	CTGGTCATGGAGTTGTACTGCAGG
Col1a1	mouse	CACCCTCAAGAGCCTGAGTC	GTTCGGGCTGATGTACCAGT
Mmp9	mouse	CTGGACAGCCAGACACTAAAG	CTCGCGGCAAGTCTTCAGAG
Mmp13	mouse	CTTCTTCTTGTTGAGCTGGACTC	CTGTGGAGGTCACTGTAGACT
Tgfb1	mouse	TTGCTTCAGTCCCACAGAGA	TGGTTGTAGAGGGCAAGGAC
Timp1	mouse	GTAAGGCCTGTAGCTGTGCC	AGGTGGTCTCGTTGATTTCT
Cd3	mouse	ATGCGGTGGAACACACTTTCTGG	GCACGTCAACTCTAACTGGT
Cd20	mouse	AACCTGCTCCAAAAGTGAACC	CCCAGGGTAATATGGAAGAGGC
Cd68	mouse	TGTGTGATCTTGCTAGGACCG	GAGAGTAACGCCTTTTTGTGA
ChIP primers	**Species**	**Forward Primer Sequence (5'->3')**	**Reverse Primer Sequence (5'->3')**
Scd1 (Novel SRE,NF-Y1,NF-Y2)	rat	AGGAGAGAGCGAGGAGCTAGT	TGCCTGAGGGTAAATGCTAATGCG
Scd2 (Novel SRE,NF-Y1,NF-Y2)	rat	ACAGCAGATTGTGCAGAG	CGTAAACTCTGGCTAGTCATTGG

TaqMan quantitation of Scd1 and Scd2 gene expression. qPCR was performed using pre-designed TaqMan primer/probe sets (Applied Biosystems) for *Scd1* (Rn00594894_g1), *Scd2* (Rn00821391_g1), and normalilsed to 36B4 (Rn03302271_gh) expression, after total RNA was extracted and cDNA was synthesized as described above.

TaqMan quantitation of miRNAs predicted to bind and regulate Lrp6 mRNA. In-silico algorithms (http://mirdb.org/miRDB/)(Wong and Wang 2015) for screening possible miRNA binding to Lrp6 mRNA 3' UTR predict possible regulation by miR-195, miR-183, miR-15b, and miR-322. Thus, qPCR was performed using pre-designed TaqMan primer/probe sets (Thermo Fisher Scientific Inc.) for miR-15b (000390), miR-126 (002228), miR-183 (002269), miR-195 (000494), and miR-322 (001076) and normalized to U6 snRNA (001973) expression after miRNA was extracted using miRNeasy kit (Qiagen) and cDNA was synthesized as described above.

Transient transfection and reporter gene assay. The mouse *Scd1* promoter (-589/+81)-luciferase and its deletion or mutation constructs, and expression vectors for SREBP-1c and β-catenin were generous gifts of investigators as indicated in Acknowledgements. BSC in 12-well plates were transfected with the promoter-reporter construct with one or a combination of the expression vectors or empty vectors using the non-lipid cationic Targefect F2 transfection reagent (Targeting Systems, San Diego, CA) at a 1:1 ratio of total amount of DNA (μg) to volume of F2 (μl). Two hours after transfection, the cells were treated with FJ9 or vehicle. After 24 h, the cells were washed in PBS and solubilized for determination of firefly luciferase activity using the Dual-Luciferase® Reporter Assay System (Promega, Madison, WI). Firefly luciferase activity was normalized to lysate total protein concentration for calculation of relative changes in the promoter activity. Lrp6 5'UTR, CR-F1, 3'UTR-F2 luciferase reporter

constructs were obtained from Prof. Jian-Ying Wang of University of Maryland. BSC in 12-well plates were transfected with the luciferase-reporter construct with one of the expression vectors using the non-lipid cationic Targefect F2 transfection reagent (Targeting Systems, San Diego, CA) at a 1:1 ratio of total amount of DNA (µg) to volume of F2 (µl). Twenty-four hours hours after transfection, the cells were treated with SCD inhibitor or vehicle. At conclusion of treatment, cell lysates were prepared and relative changes in promoter activity were determined as described above. Huh7 in 12-well plates were transfected with the luciferase-reporter construct with one of the expression vectors using the BioT reagent (Bioland Scientific, LLC, Paramount, CA) at a using a BioT (µl) to DNA (µg) ratio of 1.5:1. Five hours after transfection, the cells were treated with SCD inhibitor or vehicle. At conclusion of treatment, cell lysates were prepared and relative changes in promoter activity were determined as described above.

Chromatin immunoprecipitation (ChIP) assay. Cross-linking ChIP was performed as previously described [9] except that Dynabeads protein A or G (Life Technologies) was used to immunoprecipitate fragmented chromatin. For quantitative ChIP assay, the thermal cycle was set at 94°C 10 min, followed by 40 cycles of 30 sec at 94 °C and 1 min at 60 °C. A dissociation curve was generated to make sure of the product specificity. The final result was represented as $2^{(Ct_{Input}-Ct_{Output})}$. Anti β-catenin antibody was purchased from Cell Signaling Technology (9562), while anti SREBP-1 antibody was from Santa Cruz Biotechnology (sc-13551). For ChIP-re-ChIP, the elution was performed with 20mM DTT for 30 min at room temperature. Then the eluate was desalted with the Pierce Zeba spin desalting column, and ChIP assay with the second antibody was performed as referenced above. The qPCR primer sequences to amplify rat *Scd1 and Scd2* novel SRE/NFY1 and/or novel SRE/NFY1 and 2 sites are listed in "Primer sequences" section.

Fatty acid composition analysis. Total fatty acids were extracted from day 1 or day 7 cultured HSCs ($0.4x10^6$ cells) by the method previously described [10]. Fatty acids extracted with petroleum ether were derivatized to methyl esters for gas chromatography/mass spectrometry (GC/MS) analysis using a Hewlett-Packard selective mass detector (model 5973) connected to a gas chromarograph (model 6890) as described before [11] at the Metabolomic Core of the Southern California Research Center for ALPD and Cirrhosis. A glass capillary column BPX70 (SGE, Austin, TX) was used to separate fatty-acid derivatives using carrier gas (helium) flow rate 1 ml/min, injector temperature 250°C, and oven temperature programmed from 120 to 220°C at 5°C/min. Under these conditions, the retention time (min) and mass spectra (m/z) for fatty acids were as follows: C14:0 (3.87 min/242 m/z), C16:0 (5.76 min/270 m/z), C16:1 (n-7) (5.82 min/268 m/z), C17:0 (internal standard, 6.2 min/284 m/z), C18:0 (8.36 min/298 m/z), C18:1(n-9) (8.73 min/296 m/z), C18:1 (n-7) (8.9 min/296 m/z), C18:2 (n-6) (9.91 min/294 m/z), C20:0 (11.48 min/326 m/z), C20:4 (n-6) (14.44 min/318 m/z), C22:0 (14.86 min/354 m/z), C22:1 (15.32 min/352 m/z), and C24:0 (17.13 min/382 m/z). The quantity of individual fatty acids was calculated against the known amount of C17:0 internal standard. Fatty acid desaturation index that correlates with SCD activity was determined by the ratios of 16:1(n-7)/16:0 (palmitoleic acid/palmitic acid) and 18:1(n-9)/18:0 (oleic acid/stearic acid) [12].

Immunoblot analysis. Cell lysates were prepared by washing cells with ice-cold PBS twice, and then lysing on ice for 5 min with RIPA buffer containing freshly added protease inhibitor, PMSF, and Na3VO4 (Santa Cruz Biotechnology). After scraping cells from the plate, the lysates were transferred to a new microfuge tube and incubated on ice for 20 min, vortexed briefly, and then centrifuged at 14,000 rpm for 10 minutes at 4ºC. Supernatants were assayed for protein concentration using Coomassie (Bradford) Protein Assay Kit (Thermo Scientific), and then mixed with 6x SDS sample buffer before resolving by 6%-10% SDS-PAGE, transferring onto PVDF membrane, and immunoblotting. For immunoblotting, membrane was incubated with primary antibody in 5% non-fat-milk/1x TBS containing 0.1% Tween20 overnight at 4ºC, followed by incubation with a horseradish peroxidase-conjugated secondary antibody (Santa Cruz Biotechnology). Proteins were detected by a chemiluminescent method using Lumi-Light Western Blotting Substrate kit (Roche), and/or SuperSignal West Femto kit (Pierce).

Primary antibodies for Immunoblot	**Maker (Catalog No.)**
Acta2	Sigma-Aldrich (A2547, clone 1A4)
beta-actin	Santa Cruz Biotechnology (sc-47778; sc-1616)
p-AKT (S473)	Cell Signaling Technology (#4051)
AKT	Cell Signaling Technology (#9272S)
Non-p-beta-catenin (S33/37/T41)	Cell Signaling Technology (#4270)
p-beta-catenin (S552)	Cell Signaling Technology (#9566)

Total beta-catenin	Cell Signaling Technology (#9562)
Dvl2	Cell Signaling Technology (#3224)
Fzd1	Santa Cruz Biotechnology (sc-398082)
GAPDH	GeneTex (GT239); Santa Cruz Biotechnology (sc-32233)
GFP	Santa Cruz Biotechnology (sc-8334)
p-GSK3beta (S9)	Cell Signaling Technology (#9322S)
GSK3beta	Cell Signaling Technology (#9315S)
His	Santa Cruz Biotechnology (sc-8036)
HuR	Santa Cruz Biotechnology (sc-5261)
ILK	Millipore (MABT66)
Lamin B1	Santa Cruz Biotechnology (sc-20682)
LRP5	Cell Signaling Technology (#5731)
p-LRP6 (S1490)	Cell Signaling Technology (#2568P)
LRP6	Millipore (MABS341)
MeCP2	Abcam (ab2828)
Ran1	Santa Cruz Biotechnology (sc-1156)
SCD1	Abcam (ab19862)
Transportin 1	Sigma-Aldrich (T0825, clone D45)

ILK activity assay. ILK kinase assay was done using Akt Kinase Assay Kit (Nonradioactive) (Cell Signaling Technology, #9840) with minor modifications as described previously [13]. Immunoprecipitation with anti-ILK: Cell lysates were prepared and protein concentration measured as described above. Next, 200 µg-400 µg/400 µl of cell lysates were pre-cleared for 1 h at 4ºC with 30 µl of protein A/G plus agarose (Santa Cruz Biotechnology, sc-2003) and normal rabbit IgG (Santa Cruz Biotechnology, sc-2027). Pre-cleared lysates were then incubated with anti-ILK antibody (Millipore, MABT66) or normal rabbit IgG (control) overnight at 4ºC. 50 µl of protein A/G plus agarose was then added to lysates, followed by incubation for 2 h at 4ºC. After washing with ice-cold RIPA buffer 3 times, each sample was mixed with 2x SDS sample buffer, prior to immunoblot analysis as described above.Activity (kinase) assay: Briefly, after washing with RIPA buffer in the immunoprecipitation procedure described above, pulled-down samples were washed with 1x kinase buffer twice, and then incubated with 1x kinase buffer containing 200 µM of ATP and 1 µg of GST-fusion GSK3α/β substrates for 30 min at 30ºC. The kinase reaction was terminated by addition of 3x SDS sample buffer, prior to immunoblot analysis as described above. Phosphorylation of GSK3α/β substrates (a read-out for ILK activity) was detected by anti-phospho-GSK-3α/β (S21/9) provided in the manufacturer's kit.

LRP5/6 protein and mRNA stability assays. To assess the effect of SCD inhibition on LRP5/6 protein stability, BSCs were treated with SCD inhibitor or vehicle in the presence of cycloheximide (10 ng/ml) or its absence. Protein lysates were collected at various time points from 0 to 20-24 h after treatment, and analyzed by immunoblot analysis as described above. Densitometric analysis for LRP5/6 protein expression was done by normalizing LRP5/6 expression to respective GAPDH expression. To assess the effect of SCD inhibition on LRP5/6 mRNA transcription/stability: 1) BSCs were treated with SCD inhibitor or vehicle for 6 h, 12 h, 18 h, and 24 h in serum-free medium; 2) BSCs were treated without or with actinomycin D (1 nM) for 6 h in serum-free medium and treated with SCD inhibitor or vehicle for an additional 6 h, 12 h, 18 h, and 24 h. RNA extraction and RT-qPCR for LRP5/6 were done as described above.

Cytoplasmic and nuclear extracts. Cytoplasmic and nuclear proteins from BSC and Huh7 cells were extracted using NE-PER™ Nuclear and Cytoplasmic Extraction Kit (Thermo Scientific) as previously described [14].

Ribonucleoprotein Immunoprecipitation (RIP). RiboCluster Profiler RIP-Assay Kit (#RN1001) and Anti-ELAVL1/HuR polyclonal antibody (#RN0004P) were purchased from MBL. After Huh7 cells in 10 cm plates were treated with SCDi (20µM) concurrently with OA/SA (30µM) for 24 hours, collected and washed with cold PBS for three times, RIP assay was performed according to the manufacture's protocol. Briefly, cells were lysed

with RNase inhibitor containing lysis buffer and immunoprecipitated with IgG or HuR antibody immobilized Protein A/G plus Agarose beads for 3 hours at 4˚C. After washing four times, RNA was extracted from both Bead-Antibody RNP complex and lysates which did not undergo immunoprecipitation (the latter used for input control), and then purified with RNA Clean and Concentrator-5 Kit with DNase I treatment from Zymo Research (#R1013). The isolated RNA was reverse-transcribed to cDNA and subjected to qPCR analysis for HuR-Lrp6 mRNA RIP analysis with primer sequences designed within HuR 3'UTR: 5'-CCGGTAGCTATATGGCCTGT-3' and 5'-GCCACAGAGCGATCACATTA-3'.

Affinity purification of OA-binding proteins.

Control, stearic acid, elaidic acid and oleic acid-fixed affinity nano-beads were prepared as previously described [15]. Briefly, stearic acid, elaidic acid or oleic acid was incubated at 1 mM with equal amounts of *N*-hydroxysuccinimide and 1-ethyl-3-(3-dimethylaminopropyl) carbodiimide (Dojindo) for 2 h at room temperature and then reacted overnight with amino-modified affinity beads. For purification of OA-binding proteins, 0.2 mg of beads were equilibrated with the binding buffer (20 mM HEPES (pH7.9), 100 mM NaCl, 1 mM $MgCl_2$, 0.2 mM EDTA, 10% glycerol, 1 mM DTT, 0.2 mM PMSF, 0.1% NP40), and incubated with 0.2 mg/ml of TIC cell lysate at 4˚C for 1 h. Bound proteins were eluted with SDS-loading dye, analysed by SDS-PAGE and then visualized by silver staining (Wako). Bound proteins were subjected to in-gel digestion by trypsin, and the fragments of the peptides were analysed by ESI-MS (Waters: Synapt G2).

Computational analysis of Oleic Acid binding at the interface of Transportin-1 and Ran1. Three-dimensional structure of Transportin-1(TNPO1) at 3Å (PDB code: 2QMR) was used as a template to search for putative binding site of OA. In preparation for ligand binding studies, a robust structure model was built using homology modeling feature in Schrodinger (Schrodinger, Inc. San Diego CA). Briefly, several structural templates (PDB codes: 2QMR, 2QNA, 2w3z, 2buku etc.) were used to build the overall structure followed by loop search using prime module. Final structure model was minimized and subjected to a short molecular simulation to obtain a stereochemically acceptable structural model. Binding studies were performed using Glide (Schrodinger) and Autodock. Figures were produced using Pymol (Schrodinger, LLC. The PyMOL Molecular Graphics System, Version 1.3r1. 2010.).

Immunoprecipitation of Huh7 protein lysates to assess Transportin-1/Ran1 interaction. For IP assay, the Huh7 cells in 10cm dishes were treated with SCDi(20μM) concurrent with OA/SA (30μM) under serum –free condition for 24 hours, then the cell proteins were extracted in RIPA Lysis Buffer (Santa Cruz Biotechnology) containing 1mM PMSF and Halt protease & phosphatase inhibitor cocktail (Thermo Scientific) on ice. Then, 200μl proteins (>3mg/ml) were immunoprecipitated with a mouse monoclonal anti-Transportin 1 (T0825, clone D45) from Sigma-Aldrich with 1:50 dilution overnight in cold room, and pulled down by protein A/G plus Agorae beads (Santa Cruz Biotechnology) for 4 hours. After four times wash, the protein samples were released by SDS sample buffer with boiling. IB was performed using mouse monoclonal anti-transportin 1 antibody (T0825, clone D45, 1:1000 dilution) from Sigma-Aldrich or rabbit polyclonal antibodies against Ran1 (sc-1156, 1:1000 dilution).

Protein expression and purification for cell free system to assess Transportin-1/Ran1 binding. Transportin-1(TNPO1) protein vector (human) pPB-His-GST-TNPO1 was purchased from ABM (#PV445791). To make the construct expressing His6-GFP recombinant protein serving as control for His-tag pulldown assay, the PET28a-GFP was generated as following described. The GFP fragment was amplified from pEGFP-N1 (BD Biosciences) with two primers: GFP5E(5-TT GAA TTC ATG GTG AGC AAG GGC GAG GAG CTG-3) and GFP3S(5-TT GTC GAC CTT GTA CAG CTC GTC CAT GCC GAG-3), and then cloned into the pET28a plasmid at ECoRI and SalI sites. For His6-tagged recombinant protein expression, the vectors were transformed into E. coli BL21(DE3) cells. Expression and purification of recombinant proteins in E. coli BL21 (DE3) cells were carried out according to the manufacturer's instructions. Briefly, the purifications of His6–GFP and His-TNPO1 were performed under the native condition using Ni-NTA (Ni2+- nitrilotriacetate)–agarose columns. The protein was eluted with wash buffer plus 250mM imidazole and dialyzed against decreasing concentrations of imidazole in the same buffer as used for wash(Tris 20mM, pH=8.0, NaCl 0.5M, 1mM PMSF, and Halt protease inhibitor cocktail (Thermo Scientific). The pull-down assay was carried out in cold room as follows. Briefly, 100μl purified His-GFP and His-GST-TNPO1 protein (0.1mg/ml) were incubated with 50μl Ni-NTA resin for 2 hours. After three times wash with the same buffer, the resins were incubated with oleic acid/stearic acid (1mM) in fatty-acid free BSA solution (50mg/ml) for 6 hours. After another three times wash, the resins were incubated with 200μl Huh7 cell lysates in RIPA buffer (5.0mg/ml) on a rocking platform overnight, and then washed with wash buffer for four times. The pull-down complex was released from Ni-NTA resin together with His-tagged proteins by incubation with 100μl elution buffer (wash buffer containing 500mM imidazole) for 1hour. The samples were subjected to immunobloting with mouse monoclonal antibody against His (sc8036, 1:1000 dilution), rabbit polyclonal antibodies against Ran1 (sc-1156, 1:1000 dilution) and GFP (sc-8334, 1:1000 dilution) from Santa Cruz

Biotechnology and mouse monoclonal anti-transportin 1 antibody (T0825, clone D45, 1:1000 dilution) from Sigma-Aldrich. For OA's dose-dependent inhibition of TNPO1/Ran1 binding, 0.1 – 5 mM OA versus 0 mM (vehicle DMSO) was used as indicated.

TICs co-xenografted with Scd2 knockdown (Scd2 KD) HSCs vs. wild-type (WT) HSCs into nude mice. HSCs were isolated from Scd2f/f mice and cultured. On day 3, these HSCs were trypsinized and then treated for 4-6 days with Ad.Cre vs. Ad.LacZ to generate Scd2 KD HSCs vs. WT HSCs, respectively, after which they were re-trypsinized and harvested. Then, ~5x10e4 TICs with Scd2 KD HSCs (1:1) vs. with WT HSCs (1:1) vs. without HSCs (1:0) were co-transplanted into nude mice. Tumor volumes were assessed up to 17 days after transplantation before mice were euthanized.

DEN-induced, Western alcohol diet-promoted liver tumor development in Scd2f/f and Scd2f/f;CC mice. *Scd2f/f* vs. *Scd2f/f;CC* mice at 2 weeks of age were treated i.p. with DEN (Sigma, 25 mg/kg) and then fed the Western alcohol diet (Dyets, Inc. #710362) high in cholesterol and Saturated fat for 4 months, after which mice were euthanized for assessment of tumor incidence, multiplicity and volume.

Acknowledgements. We thank Peter Edwards (UCLA) for Scd1 promoter-reporter constructs, Michael Kahn (USC) for ICG-001, Timothy Osborne (UC Irvine) for SREBP-1c expression vector, Randall Moon (University of Washington) for β-catenin expression vector, Calvin Kuo (Stanford University) for adenovirus expressing DKK-1, Jiaohong Wang, Stephanie Pan, Yuntao Wang, and Raul Lazaro for technical support from the Southern California Research Center for ALPD and Cirrhosis, Deborah L. Berry for technical support at the Histopathology and Tissue Shared Resource of Lombardi Comprehensive Cancer Center of Georgetown University, and Kenneth Dorko for technical support at the Department of Pharmacology, Toxicology and Therapeutics Cell Isolation Core of the University of Kansas Medical Center.

Supplemental References

1. Cheng JH, She H, Han YP, et al. Wnt antagonism inhibits hepatic stellate cell activation and liver fibrosis. Am J Physiol Gastrointest Liver Physiol 2008;294:G39-49.
2. Fujii N, You L, Xu Z, et al. An antagonist of dishevelled protein-protein interaction suppresses beta-catenin-dependent tumor cell growth. Cancer Res 2007;67:573-9.
3. Emami KH, Nguyen C, Ma H, et al. A small molecule inhibitor of beta-catenin/CREB-binding protein transcription [corrected]. Proc Natl Acad Sci U S A 2004;101:12682-7.
4. Chen CL, Tsukamoto H, Liu JC, et al. Reciprocal regulation by TLR4 and TGF-β in tumor-initiating stem-like cells. J Clin Invest 2013;123:2832-49.
5. Bansal S, Berk M, Alkhouri N, et al. Stearoyl-CoA desaturase plays an important role in proliferation and chemoresistance in human hepatocellular carcinoma. J Surg Res 2014;186:29-38.
6. Strom SC, Pisarov LA, Dorko K, et al. Use of human hepatocytes to study P450 gene induction. Methods Enzymol 1996;272:388-401.
7. Kim JH, Sohn BH, Lee HS, et al. Genomic predictors for recurrence patterns of hepatocellular carcinoma: model derivation and validation. PLoS Med 2014;11:e1001770.
8. Sung CK, She H, Xiong S, et al. Tumor necrosis factor-alpha inhibits peroxisome proliferator-activated receptor gamma activity at a posttranslational level in hepatic stellate cells. Am J Physiol Gastrointest Liver Physiol 2004;286:G722-9.
9. Yang MD, Chiang YM, Higashiyama R, et al. Rosmarinic acid and baicalin epigenetically derepress peroxisomal proliferator-activated receptor γ in hepatic stellate cells for their antifibrotic effect. Hepatology 2012;55:1271-81.
10. Lowenstein JM, Brunengraber H, Wadke M. Measurement of rates of lipogenesis with deuterated and tritiated water. Methods Enzymol 1975;35:279-87.
11. Xu J, Lee WN, Phan J, et al. Lipin deficiency impairs diurnal metabolic fuel switching. Diabetes 2006;55:3429-38.
12. Attie AD, Krauss RM, Gray-Keller MP, et al. Relationship between stearoyl-CoA desaturase activity and plasma triglycerides in human and mouse hypertriglyceridemia. J Lipid Res 2002;43:1899-907.
13. Tabe Y, Jin L, Tsutsumi-Ishii Y, et al. Activation of integrin-linked kinase is a critical prosurvival pathway induced in leukemic cells by bone marrow-derived stromal cells. Cancer Res 2007;67:684-94.
14. Xu J, Chi F, Guo T, et al. NOTCH reprograms mitochondrial metabolism for proinflammatory macrophage activation. J Clin Invest 2015;125:1579-90.
15. Kabe Y, Ohmori M, Shinouchi K, et al. Porphyrin accumulation in mitochondria is mediated by 2-oxoglutarate carrier. J Biol Chem 2006;281:31729-35.